A-014
J. Chem. Thermodynamics **1978**, 10, 507–522

CrAs: heat capacity, enthalpy increments, thermodynamic properties from 5 to 1280 K, and transitions[a]

R. BLACHNIK,[b] and G. KUDERMANN,[c]
Anorganisch-Chemisches Institut der Technischen Universität Clausthal, Clausthal-Sellerfeld, B.R.D.

F. GRØNVOLD,
Department of Chemistry, University of Oslo, Blindern, Oslo 3, Norway

A. ALLES,[d] B. FALK,[e] and E. F. WESTRUM, JR
Department of Chemistry, University of Michigan, Ann Arbor, Michigan 48109, U.S.A.

(*Received 7 March 1977*)

The heat capacity of chromium arsenide has been measured by adiabatic calorimetry from 5 to 1050 K and enthalpy increments have been taken over the range 875 to 1280 K with respect to 298.15 K by drop calorimetry. The heat capacity shows a distinct bell-shaped transition with a peak at 259.9 K related to the disappearance of antiferromagnetic helical ordering on heating. The enthalpy and entropy of this transition are 177 cal_{th} mol^{-1} and 0.69 cal_{th} K^{-1} mol^{-1}, respectively. At 1170 K another transition is observed related to the phase change from the MnP- to the NiAs-type structure. The enthalpy and entropy of the latter gradual transition are 280 cal_{th} mol^{-1} and 0.22 cal_{th} K^{-1} mol^{-1}, respectively. Thermodynamic functions have been evaluated and the values of C_p, $\{S°(T)-S°(0)\}$,-$\{G°(T)-H°(0)\}/T$ at 298.15 K are 12.501, 15.40, and 6.990 cal_{th} K^{-1} mol^{-1} and 16.09, 32.53, and 19.86 cal_{th} K^{-1} mol^{-1} at 1000 K.

1. Introduction

Chromium monoarsenide has been extensively studied by X-ray and neutron diffraction, magnetic susceptibility, and magnetization techniques,[1–17] and two solid-state transitions have been described. The thermodynamic properties of CrAs are largely

[a] The low-temperature measurements completed at the University of Michigan were supported in part by the Chemical Thermodynamics Program, Chemistry Section, National Science Foundation under Contract No. GP-42525X. The high-temperature measurements are part of the Ph.D. Thesis by G. Kudermann and were supported by Grafög.

[b] Present address: Gesamt hochschule Siegen, F.B. Chemie, D-5900 Siegen 21, B.R.D.
[c] Present address: Vereinigte Aluminium-Werke AG, Leichtmetall-Forschungs-institut, Gerichberg-48, 53 Bonn 1, B.R.D.
[d] Present address: Dep. de Quimica, Universidade Federal de Santa Catarina, Cidade Universitaria, 88000 Florianopolis, Brazil.
[e] Present address: Thermochemistry, Chemical Center, University of Lund, P.O.B. 740, S-220 07 Lund 7, Sweden.

0021-9614/78/0601-0507 $02.00/0

unknown, however, except for the heat-capacity measurements by Kazama and Watanabe[11] in the region 180 to 280 K. The present investigation has been undertaken to improve and extend the earlier heat capacities thereby providing thermodynamic data for CrAs over the stability ranges of the solid phases, and in particular, to explore the detailed trends in the regions of both the low-temperature transformation and the higher-temperature transition.

X-Ray studies show CrAs to have a structure of the orthorhombic MnP-type at 300 K.[1,3–6,9,10,12,13,16] The presence of a homogeneity range on the chromium-rich side was claimed for this phase by Boller *et al.*[6,13] while other authors[12,16] consider that exact 1—1 stoichiometry is characteristic of CrAs and other MnP-type phases. The MnP-type structure can be derived from the NiAs-type structure by shifting the non-metal atoms slightly along the c-axis and displacing the metal atoms normal to the c-axis. High-temperature X-ray data have shown that the c/b axial ratio gradually approaches the orthohexagonal $\sqrt{3}$ at higher temperature. Watanabe *et al.*[9] reported this to occur at 800 K, while Boller and Kallel[13] considered the approach to $\sqrt{3}$ as fortuitous and not indicative of a transition to the NiAs-type structure since they observed reflections forbidden in the NiAs space group, $P6_3/mmc$, even at 1100 K. According to Selte and Kjekshus[14] and Selte,[16] the structure is still orthorhombic at 1120 K, *i.e.* above the maximum temperature used by Boller and Kallel[13] and becomes hexagonal first at (1173 ± 20) K.

According to Haraldsen and Nygaard[2] the magnetic susceptibility of CrAs increases steadily over the region 80 to 600 K, indicating the enhanced population of higher magnetic states. Yuzuri[3] found a peak in the susceptibility at 820 K which was taken to imply an antiferromagnetic-to-paramagnetic transition in this region, while Selte and Kjekshus[14] observed a further small increase in susceptibility in the region 800 to 970 K. Above 300 K one might then expect to encounter an excess heat capacity due to the population of excited electronic states in chromium and also a thermal effect accompanying the transformation from the MnP- into the NiAs-type structure.

Below 300 K a sudden structural change occurs in CrAs, which is related to a double-helical spin ordering with spiral propagation in the *ab*-plane.[9,10,12,13,16,17] Watanabe *et al.*[9,10] reported that this occurred at about 280 K while discontinuities in the lattice constants and anomalies in electrical resistivity and thermoelectric power occurred at 265 K. Selte *et al.*[12,16] observed the transition to go to completion at 272 K on heating while the spiral structure reappeared at 261 K on cooling. According to Boller and Kallel[13] the transformation takes place in the range 190 to 240 K and shows hysteresis and supercooling effects. The volume contraction on heating is accompanied by shortening the distance of one additional Cr—Cr contact considerably below the value $r_c = 318$ pm which according to Mott[18,19] and Goodenough[20] is a critical interatomic distance for the localized-collective electron behavior. The results were discussed[13] in terms of a suggested band model, but the validity of the model is questionable since both the electrical-resistivity results by Kazama and Watanabe[10,11] and the neutron-diffraction results of Selte *et al.*[12,16] indicate that the phase below the transition is metallic also.

2. Experimental

SAMPLE PREPARATION

The synthesis was made at Clausthal from high-purity elements. Chromium, obtained from Johnson Matthey Metals Ltd., London, had mass fraction 10^{-5} of metallic impurities. The arsenic was 99.9999 mass per cent pure, crystalline material from Preussag, F.R.G. The stoichiometric mixture of the elements was first heated for 2 d at 920 K and then for 5 d at 1170 K. The product was then crushed and heated for 10 d at 1120 K. The procedure was repeated again since arsenic was still observed in the tube. Even so, 0.3 mass per cent of arsenic remained unreacted. This corresponds to a composition $CrAs_{0.995}$. The sample was examined by X-ray diffraction, using KCl as calibrating substance, a(293 K) = 629.19 pm. The lattice parameters observed were $a = (564.7 \pm 0.2)$ pm, $b = (346.0 \pm 0.2)$ pm, and $c = (620.7 \pm 0.3)$ pm, in good agreement with the results by Hollan *et al.*[4] and by Selte and Kjekshus.[14]

CALORIMETRIC TECHNIQUE

5 to 350 K, *University of Michigan.* The heat capacity of CrAs was measured in the Mark II adiabatic calorimetric cryostat described elsewhere.[22] A gold-plated copper calorimeter (W-52) with a volume of 59 cm^3 was used. Temperatures were measured with a capsule-type platinum resistance thermometer (A-5) located in a central well in the calorimeter. The calorimeter was loaded with sample, and evacuated, and helium gas was added at 7.2 kPa pressure to provide thermal contact between sample and calorimeter. It was then sealed, placed in the cryostat, and cooled. Temperatures are judged to correspond to IPTS-68 within 0.02 K from 4 to 350 K. Measurements of mass, resistance, potential, current, and time were referred to standardizations and calibrations performed at the U.S. National Bureau of Standards.

The heat capacity of the empty calorimeter was determined in a separate series of experiments. The heat capacity of the 136.49 g sample represented from 80 to 90 per cent of the total. Small corrections were applied for temperature excursions of the shields from the calorimeter temperature and for "zero drift" of the calorimeter temperature. Further small corrections were applied for differences in amounts of indium + tin solder, helium gas, and Apiezon-T grease.

300 to 1050 K, *University of Oslo.* The calorimetric apparatus and measuring technique have been described.[23] The calorimeter was intermittently heated, and surrounded by electrically heated and electronically controlled adiabatic shields. The substance was enclosed in an evacuated and sealed vitreous-silica tube of about 50 cm^3 volume, tightly fitted into the silver calorimeter. A central well in the tube served for the heater and platinum resistance thermometer.

The platinum resistance thermometer for the high-temperature heat-capacity calorimeter was calibrated locally at the ice, steam, zinc, and antimony points. Temperatures are judged to correspond to IPTS-68 within 0.05 K from 300 to 900 K and within 0.2 K at 1050 K. The accuracy in the energy inputs is about 0.03 per cent. The heat capacity of the empty calorimeter, including the vitreous-silica container, was determined in a separate series of experiments. The heat capacity of the 139.20 g sample represented about 55 per cent of the total. Corrections were applied for

"zero drift" of the calorimeter and for differences in the masses of the vitreous silica containers.

875 to 1280 K *enthalpy increments relative to* 298.15 K, *University of Oslo.* An aneroid drop calorimeter operating in air was used in the determinations. Details of the construction have been described[24] together with results obtained for a IV. Calorimetry Conference sample of α-Al_2O_3.

About 5 g of CrAs was sealed in a vitreous-silica container which again was placed in a (platinum + 10 per cent by mass of rhodium) container in a vertical tube furnace. The equilibrated sample assembly was hoisted into the silver calorimeter with electrically heated adiabatic shields, and the temperature increment of the calorimeter measured with a quartz thermometer (HP Model 2801A). The sample temperature in the furnace was measured with a Pt-to-PtRh (10 per cent Rh by mass) thermocouple. Uncertainty in the sample temperature, estimated to be about 1 K at 1300 K, represents the main source of error in the enthalpy determinations.

3. Results

The experimental heat capacities from both the low- and high-temperature ranges are presented in table 1. These are arranged in chronological order so that temperature increments used may usually be inferred from differences in mean temperatures. The enthalpy increments from drop calorimetry are presented in table 2, and may be represented by the equation:

$$\{H(T)-H(298.15\ \mathrm{K})\}/\mathrm{cal_{th}\ mol^{-1}} = 276.877X^{-1}-130.120 +21112.47X-13816.1X^2+8150.7X^3, \quad (1)$$

in which $X = (T/\mathrm{K}-500.5)/800.5$ over the region 700 to 1180 K.† The deviations of the experimental points are represented by a standard deviation of 0.1 per cent. A comparison of both enthalpies and heat capacities in the overlap region is given in table 3. The low-temperature heat capacities are displayed in figure 1 with details of the low-temperature transition shown in figure 2 and the high-temperature results in figure 3. The standard deviation of a single heat-capacity measurement is less than 1 per cent from 8 to 25 K, 0.1 per cent from 25 to 300 K, and 0.2 per cent from 300 to 350 K. In the higher-temperature region it is 0.5 per cent. For the heat capacity derived from enthalpy increments above 1180 K, it is several per cent.

LOW-TEMPERATURE TRANSITION

The transition was mapped with four series of determinations. Determinations of series V and VIII were made only after the sample had been taken to 60 K, and determination of series XII, XIII, and XV were made after the sample had been taken to 4 K. For series V and VIII the sample was first cooled to 240 K and after approximately 1 h determinations were begun. Equilibrium was reached 25 to 40 min after each energy input. For series XII, XIII, and XV through the transition, the sample was cooled to 200 K and then heated slowly over 5 h to 250 K. The automatic controllers were offset to compensate for quasi-adiabatic drift, and for the determin-

† Throughout this paper $\mathrm{cal_{th}} = 4.184$ J; atm = 101.325 kPa.

TABLE 1. Heat capacity of CrAs

(cal_{th} = 4.184 J, M = 126.918 g mol^{-1})

Low-temperature results (Ann Arbor)

T/K	C_p/cal_{th} K^{-1} mol^{-1}
Series I	
165.51	9.915
172.14	10.157
178.65	10.377
185.04	10.589
191.34	10.793
197.53	10.98
204.45	11.19
212.07	11.42
219.86	11.67
227.80	11.91
235.58	12.19
243.21	12.51
250.66	12.98
256.57	23.45
260.27	37.78
265.15	14.18
272.31	12.63
Series II	
268.25	12.67
274.98	12.55
285.56	12.47
295.75	12.51
305.90	12.56
315.97	12.61
326.00	12.69
336.01	12.76
343.54	12.80
348.07	12.81
Series III	
65.85	3.730
73.84	4.458
80.74	5.075
88.65	5.743
97.53	6.403
105.65	6.960
113.87	7.479
122.22	7.973
131.35	8.466
141.17	8.923
150.42	9.332
159.34	9.695
167.98	10.008
176.39	10.298
Series IV	
ΔH Detn.	A
ΔH_t Detn.	B
322.53	12.65
Series V	
237.46	12.24
241.49	12.41
243.77	12.51
246.03	12.59
248.27	12.73
250.50	12.85
252.70	13.06
254.85	13.72
256.73 [a]	18.56
258.02 [a]	34.46
258.88 [a]	43.99
259.65 [a]	42.50
260.49 [a]	37.11
261.47 [a]	30.16
262.79 [a]	19.63
264.62	13.87
266.76	12.97
268.99	12.48
271.26	12.43
273.53	12.42
277.50	12.43
283.19	12.42
288.86	12.44
Series VI	
ΔH_t Detn.	C
236.07	12.182
296.81	12.49
Series VII	
ΔH_t Detn.	
238.18	12.24
300.21	12.53
Series VIII	
242.57	12.42
244.88	12.54
247.14	12.64
249.39	12.76
251.60	12.91
253.77	13.20
255.15	13.46
255.81	14.07
256.44 [a]	15.24
256.95 [a]	16.70
257.31 [a]	18.86
257.58 [a]	21.27
257.88 [a]	27.72
258.18 [a]	26.87
258.42 [a]	30.34
258.64 [a]	40.99
258.93 [a]	43.76
259.24 [a]	40.62
259.51 [a]	39.70
259.77 [a]	41.31
260.01 [a]	41.35
260.84 [a]	42.58
261.86 [a]	29.54
263.56	16.27
265.68	13.44
267.83	12.64
270.05	12.44
272.29	12.41
Series IX	
4.45	0.009
5.19	0.012
6.37	0.015
7.50	0.020
8.84	0.027
9.99	0.033
11.09	0.041
12.19	0.049
13.50	0.062
14.89	0.081
16.34	0.103
17.97	0.137
19.80	0.184
21.68	0.243
23.63	0.318
25.94	0.416
28.17	0.538
30.08	0.015
32.40	0.798
35.93	1.048
39.79	1.347
43.26	1.636
46.61	1.922
Series X	
30.13	0.652
33.02	0.842
36.35	1.080
40.52	1.407
44.78	1.767
49.17	2.161
53.55	2.563
57.72	2.956
61.58	3.326
67.39	3.875
Series XI	
ΔH_t Detn.	E
234.91	12.148
289.64	12.43
Series XII	
251.90	12.91
255.19	13.83
257.07	15.37
257.44	18.41
257.49	22.00
258.10	26.35
258.37	30.53
258.60	34.62
258.81	37.69
259.01	40.23
259.20	42.04
259.38	43.55
Series XIII	
260.27	43.42
260.45	42.76
260.63	41.86
260.82	40.61
261.01	39.55
261.21	38.38
261.42	36.75
261.63	35.41
261.85	33.79
262.08	32.13
262.33	29.59
262.59	27.19
262.89	23.11
263.24	18.21
263.65	15.91
264.10	14.82
264.57	14.50
265.04	13.78
267.00	13.04
271.07	12.39
277.32	12.42
285.64	12.42
292.71	12.45
299.74	12.52
308.52	12.55
Series XIV	
317.26	12.64
326.29	12.67
336.47	12.71
345.24	12.80

TABLE 1—*continued*

T/K	C_p/cal$_{th}$ K^{-1} mol^{-1}	T/K	C_p/cal$_{th}$ K^{-1} mol^{-1}	T/K	C_p/cal$_{th}$ K^{-1} mol^{-1}	T/K	C_p/cal$_{th}$ K^{-1} mol^{-1}
			Low-temperature results (Ann Arbor)				
Series XV		257.93	23.50	259.12	41.39	260.04	44.26
251.94	12.90	258.23	28.06	259.31	42.85	260.22	43.50
255.31	13.94	258.48	32.29	259.50	43.75	260.41	43.29
257.16	15.77	258.91	35.97	259.68	44.30		
257.58	19.38	258.92	39.04	259.86	44.47		
			Higher temperature results (Oslo)				
Series I		555.70	14.24	Series V		751.28	14.96
331.79	12.83	569.80	14.21	872.95	15.54	766.19	15.01
345.85	12.97	583.94	14.28	888.27	15.57	781.11	15.09
359.87	13.08			903.66	15.67	796.08	15.12
373.87	13.18	Series III		919.11	15.71	811.12	15.17 [b]
387.84	13.27	303.67	12.44	934.62	15.79	826.16	15.39
401.79	13.38	317.81	12.63	950.20	15.83	841.16	15.45 [b]
415.72	13.48	331.83	12.78	965.86	15.91	856.20	15.63 [b]
429.66	13.56	345.76	12.96	981.59	16.00	871.36	15.59 [b]
443.60	13.65			997.40	16.08		
		Series IV		1013.31	16.16	Series VII	
Series II		579.77	14.34	1029.29	16.23	800.25	15.17
457.80	13.66	593.90	14.33	1045.42	16.28	815.33	15.20
471.71	13.78	608.08	14.36			831.44	15.27
485.64	13.85	622.36	14.42	Series VI		845.51	15.46 [b]
499.60	13.89	636.70	14.52	692.31	14.66	860.53	15.69 [b]
513.59	13.94	651.09	14.54	706.96	14.82	875.65	15.48
527.61	14.05	665.53	14.60	721.66	14.87	890.96	15.50
541.64	14.14	680.04	14.62	736.43	14.90	906.38	15.56

[a] These determinations made before cooling the sample to liquid-helium temperatures show some scattering and a displacement of the peak of transition toward lower temperatures.

[b] Values in the α- to β-quartz region not used in the curve fitting.

TABLE 2. Enthalpy increments above 298.15 K obtained in the drop calorimeter (Oslo) (cal$_{th}$ = 4.184 J, M = 126.918 g mol^{-1})

T/K	$H°(T) - H°(298.15\ K)$/cal$_{th}$ mol^{-1}	$10^2\Delta H$[a]/cal$_{th}$ mol^{-1}	T/K	$H°(T) - H°(298.15\ K)$/cal$_{th}$ mol^{-1}	$10^2\Delta H$[a]/cal$_{th}$ mol^{-1}
875.3	8158	+0.05	1182.8	13194	−0.04
875.6	8147	−0.13	1204.3	13514	[b]
984.6	9850	+0.05	1204.2	13517	[b]
984.6	9848	+0.03	1223.8	13778	[b]
1074.9	11304	+0.02	1223.7	13762	[b]
1074.9	11295	−0.07	1280.2	14663	[b]
1183.6	13222	+0.06			

[a] Percentage deviation from smoothed curve.

[b] Unfitted results in transition region.

TABLE 3. Comparison of results taken by adiabatic and drop calorimetry in the region 875 to 1050 K
(cal_{th} = 4.184 J, M = 126.918 g mol^{-1})

Calorimeter	$C_p/cal_{th}\ K^{-1}\ mol^{-1}$				$\{H°(T) - H°(298.15\ K)\}/kcal_{th}\ mol^{-1}$			
T/K	900	950	1000	1050	900	950	1000	1050
Drop	15.36	15.52	15.84	16.34	8.53	9.30	10.09	10.89
Adiabatic	15.60	15.84	16.09	16.31	8.58	9.37	10.17	10.98

ations in the transition region both the energy inputs and drift times (30 min) were kept constant. The scattering in the two first series may be due to hysteresis and failure to achieve equilibrium. It is also interesting that the heat-capacity maximum moved to a higher temperature after the sample was taken to 4 K. The heat capacity rises to a rounded peak and then drops smoothly but gradually. Hence, the higher-temperature slope of the transition curve should be populated with experimental points in contrast to that of typical magnetic-disordering transitions. The shoulder on the high-temperature side of the transition is another peculiar feature. The enthalpy determinations through the transition region are summarized in table 4. A cooling curve taken at a rate of about 0.09 K min^{-1} is illustrated in figure 4. The rate of cooling slows

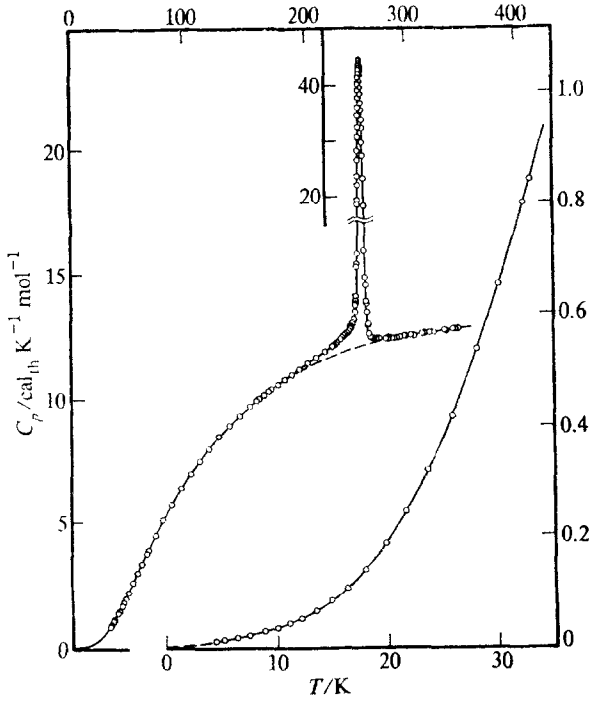

FIGURE 1. Low-temperature heat capacity of CrAs. ○, experimental results; —— —— ——, estimated non-transitional heat capacity.

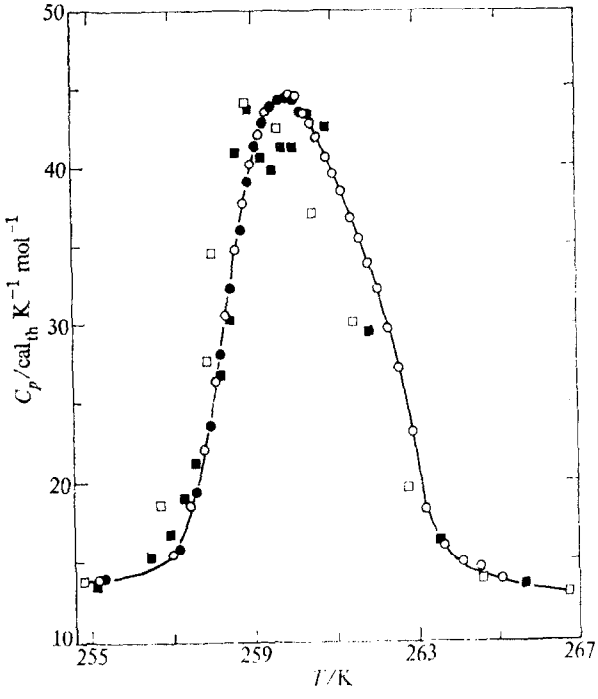

FIGURE 2. Heat capacity of CrAs in the low-temperature transition region. The scattered values Series V (□) and Series VIII (■) identify measurements made before cooling the sample to liquid-helium temperature; subsequent values are those of Series XIII (○) and Series XV (●).

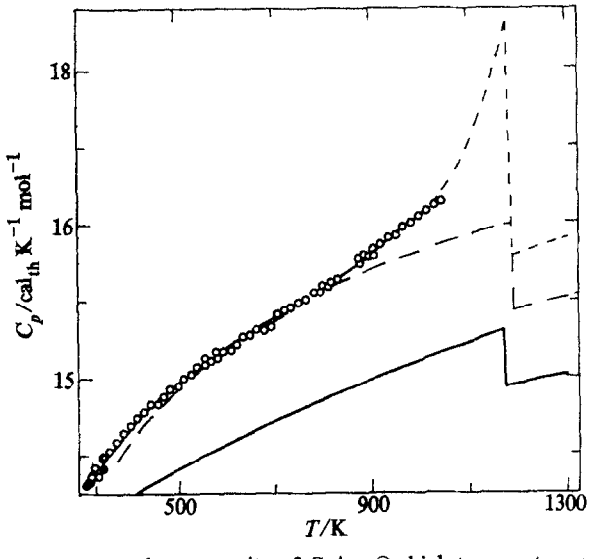

FIGURE 3. Higher-temperature heat-capacity of CrAs. ○, high-temperature adiabatic calorimetry values; ●, overlapping low-temperature adiabatic-calorimetry values; – – –, curve consistent with drop-calorimetry results; ———, estimated lattice heat capacity; ——— ———, lattice plus Schottky heat-capacity contribution (this curve represents also the non-transitional heat capacity for the high-temperature transition).

TABLE 4. Enthalpy of transition determinations for CrAs
($cal_{th} = 4.184$ J, $M = 126.918$ g mol^{-1})

Designation	T_1 / K	T_2 / K	$H(T_2) - H(T_1)$ / cal_{th} mol^{-1}	$H(295\text{ K}) - H(240\text{ K})$ / cal_{th} mol^{-1}
Detn. B	238.26	318.15	1140.80	828.6
Detn. C	239.89	292.34	795.19	827.1
Detn. D	240.61	295.10	821.64	830.4
Detn. E	238.60	287.64	753.77	828.4
				Mean: (828.6 ± 1.6)
			Non-transitional enthalpy: 652	
				ΔH_t: 177

perceptively near 253.5 K and persists to 250 K where it again increases and soon returns to the initial rate. The sample does undercool as might be expected for a first-order transition. From the curve, the ΔH_t is estimated to be 140 cal_{th} mol^{-1}, which accounts for approximately 80 per cent of the value determined by the heat-capacity measurements.

HIGHER-TEMPERATURE TRANSITION

The adiabatic heat-capacity measurements were performed up to 1050 K and the drop-calorimetric enthalpy determinations from 875 to 1280 K. The measured heat capacities are considered to be more reliable than those derived from enthalpy determinations and are chosen for integration in the region of overlap. see table 3.

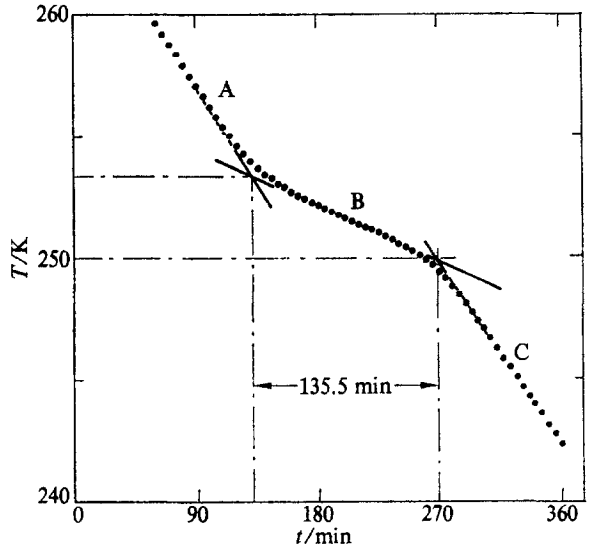

FIGURE 4. Cooling curve for CrAs. The dashed lines indicate the extrapolations made to evaluate the enthalpy of transition.

TABLE 5. Thermodynamic functions of CrAs
(cal_{th} = 4.184 J, M = 126.918 g mol^{-1})

T / K	C_p / $cal_{th}\ K^{-1}\ mol^{-1}$	$S°$ / $cal_{th}\ K^{-1}\ mol^{-1}$	$H°(T) - H°(0)$ / $cal_{th}\ mol^{-1}$	$-\{G°(T) - H°(0)\}/T$ / $cal_{th}\ K^{-1}\ mol^{-1}$
5	0.011	0.010	0.014	0.007
10	0.033	0.023	0.116	0.011
15	0.082	0.044	0.387	0.018
20	0.189	0.081	1.035	0.029
25	0.376	0.141	2.411	0.045
30	0.645	0.233	4.930	0.068
35	0.980	0.356	8.970	0.100
40	1.364	0.512	14.815	0.142
45	1.785	0.697	22.675	0.193
50	2.233	0.908	32.710	0.253
60	3.174	1.397	59.72	0.402
70	4.118	1.958	96.20	0.584
80	5.012	2.567	141.90	0.793
90	5.834	3.205	196.20	1.025
100	6.578	3.859	258.32	1.276
110	7.247	4.518	327.50	1.541
120	7.848	5.175	403.03	1.816
130	8.389	5.825	484.26	2.100
140	8.875	6.465	570.6	2.389
150	9.314	7.092	661.6	2.681
160	9.713	7.706	756.8	2.976
170	10.080	8.306	855.8	3.272
180	10.423	8.892	958.3	3.568
190	10.747	9.464	1064.1	3.864
200	11.059	10.024	1173.2	4.158
210	11.363	10.571	1285.3	4.450
220	11.666	11.106	1400.4	4.741
230	11.980	11.631	1518.7	5.028
240	12.338	12.149	1640.2	5.315
250	12.805	12.661	1765.7	5.598
255	13.760	12.921	1831.4	5.739
259.86 [a]	(44.470)	13.376	1948.7	5.877
260	44.300	13.398	1954.5	5.881
265	13.870	13.924	2092.3	6.029
270	12.421	14.146	2156.5	6.177
280	12.415	14.616	2280.6	6.471
290	12.453	15.05	2404.9	6.759
300	12.515	15.48	2529.7	7.043
350	12.829	17.43	3163.3	8.390
400	13.34	19.19	3821.5	9.634
450	13.64	20.79	4497.6	10.795
500	13.94	22.24	5188.2	11.858
550	14.17	23.57	5890.0	12.861
600	14.35	24.81	6602.8	13.808
650	14.55	25.97	7277.8	14.770
700	14.75	27.05	8057.7	15.544
750	14.96	28.07	8799.9	16.340
800	15.15	29.05	9552.5	17.109
850	15.37	29.98	10315.4	17.844
900	15.60	30.86	11089	18.538
950	15.85	31.71	11876	19.210

TABLE 5—*continued*

T / K	C_p / $cal_{th}\ K^{-1}\ mol^{-1}$	$S°$ / $cal_{th}\ K^{-1}\ mol^{-1}$	$H°(T) - H°(0)$ / $cal_{th}\ mol^{-1}$	$-\{G°(T) - H°(0)\}/T$ / $cal_{th}\ K^{-1}\ mol^{-1}$
1000	16.09	32.53	12674	19.855
1100	17.03	34.10	14323	21.079
1180	(18.4) [b]	35.34	15754	21.989
1180	(15.6)	35.34	15754	21.99
1200	(15.6)	35.60	16066	22.21
1300	(15.8)	36.86	17606	23.29
273.15	12.412	14.308	2195.6	6.270
298.15	12.501	15.40	2506.6	6.990

[a] Peak of low temperature transition.
[b] Peak of high-temperature transition.

Heat capacities derived from enthalpy measurements increased continuously in the range 1050 to 1180 K. The mean heat capacity between 1180 and over the range to 1204 K is, however, much lower than below 1180 K and the transition temperature is therefore taken as (1180 ± 10) K.

Above the transition the enthalpy values show some scattering and indicate that the heat capacity drops to as low as 14 $cal_{th}\ K^{-1}\ mol^{-1}$ at 1210 K and then rises to 16.5 $cal_{th}\ K^{-1}\ mol^{-1}$ at 1280 K. In view of the uncertainty in the derived heat-capacity values we chose to neglect the dip at 1210 K and estimated the mean heat capacity in this region to be about 15.7 $cal_{th}\ K^{-1}\ mol^{-1}$, which is consistent with the total enthalpy up to 1280 K (see end of table 5 and figure 3).

THERMODYNAMIC FUNCTIONS

The experimental heat capacities for the low- and high-temperature series were fitted to polynomials in reduced temperature by the method of least squares, and integrated to yield values of thermodynamic functions at selected temperatures. Below 10 K the heat capacities were smoothed and extrapolated with a plot of C_p/T against T^2 and the functions evaluated by extrapolation. The coefficient γ of the electronic heat capacity was found to be $\gamma = (1.8 \pm 0.2) \times 10^{-3}\ cal_{th}\ K^{-2}\ mol^{-1}$. Within the low-temperature transition region the values were read from a large-scale plot and the thermodynamic functions were calculated by numerical integration of the curves with Simpson's rule. The enthalpy increments were fitted to the function:

$$H°(T) - H°(298.15\ K) = a/T + b + cT + dT^2 + eT^3, \qquad (2)$$

in the region 900 to 1180 K. The heat-capacity curve obtained by differentiation of this function was joined smoothly at 1050 K with the heat-capacity curve from adiabatic calorimetry. This smoothed curve was then integrated to yield thermodynamic functions between 900 and 1180 K. The enthalpy increments in the high-temperature transition region were plotted and a smooth curve was drawn through the points. The heat capacity and thermodynamic functions were then calculated by hand. The thermodynamic functions from 5 to 1300 K are presented in table 5. Above 100 K the precision of the values in this table (taken as twice the standard deviation) is 0.2 per cent for the heat capacity, and 0.15 per cent for the thermodynamic

functions over the low-temperature range; over the high-temperature range they are 0.4 and 0.2 per cent, respectively.

4. Discussion

LOW-TEMPERATURE TRANSITION

In attempting to ascertain the thermodynamics of the magnetic-ordering transition, we note that apparently none of the MnP-type pnictides is diamagnetic.[16] This makes it difficult to find an adequate lattice heat-capacity model among the isostructural analogs of CrAs such as FeAs, CoAs, MnAs, and FeP. A further complication is that Schottky-type contributions to the heat capacity are anticipated above the transition. In order to estimate the lattice contribution, the heat-capacity curve far below T_t was smoothly joined with the C_p-curve above the transition. The estimated lattice heat capacity is displayed in figure 1 by the dashed line. With this lattice estimate we find $\Delta S_t = 177\ \mathrm{cal_{th}\ K^{-1}\ mol^{-1}}$ and $\Delta H_t = 0.69\ \mathrm{cal_{th}\ mol^{-1}}$. Kazama and Watanabe[11] reported $T_t = 265$ K and $\Delta H_t = 124\ \mathrm{cal_{th}\ mol^{-1}}$ for this transition as determined by continuous heating adiabatic calorimetry. The heat capacities shown in the figure by Kazama and Watanabe,[11] which can be read to only about 5 per cent, are in reasonable accord with the present results. The discrepancies in ΔH_t and T_t stem most probably from the different methods used: dynamic versus equilibrium measurements—but differences in the non-transitional heat capacity chosen, as well as differences in the nature of the samples are presumably also of importance.

Kazama and Watanabe[11] found excellent agreement between the observed entropy of transition, $\Delta S_{obs} = 0.47\ \mathrm{cal_{th}\ K^{-1}\ mol^{-1}}$, and that estimated from the sudden drop in sublattice magnetization as determined by neutron diffraction, $\Delta S_{calc} = 0.48\ \mathrm{cal_{th}\ K^{-1}\ mol^{-1}}$. The latter value was derived by fitting the reduced magnetization to Brillouin-function behavior for spin quantum number $S = 1$, which resulted in a critical magnetization $\sigma_c = 0.55$ at the transition temperature (264 K). The corresponding gain in entropy can then be found in existing tabulations.[25] The presently observed transitional entropy is considerably larger, however, but no exact correspondence is to be expected due to the change in bonding energy and volume in the transition.

The value of the transition temperature, $T_t = (259.86 \pm 0.05)$ K, is not within the broad temperature range from 240 to 190 K assigned to the occurrence of the transition by Boller and Kallel[13] and is also much lower than the approximate value of 280 K reported by Watanabe *et al.*[9] from neutron-diffraction studies. As reported in the experimental section and illustrated by figure 2, some scattering and a slightly lower heat-capacity maximum was obtained from results taken before cooling the sample to 4 K. This is an indication of the dependence of the thermal behavior upon thermal history.

X-ray crystallographic,[13] neutron diffraction[12,13] and magnetization[10] studies have shown that the transition is of first order. The magnetization studies seem of doubtful validity in this connection, however, as the investigations by Sobczak and Boller[15] and Sobczak[26] have shown that the adjacent more chromium-rich phase, Cr_4As_3, becomes ferromagnetic below 250 K ($T_c = 246$ K for $Cr_{0.59}As_{0.41}$). Thus,

any change in magnetization of CrAs connected with the low-temperature transition is overshadowed by the presence of a small amount of the Cr_4As_3 phase.

The shape of the heat-capacity curve suggests that the transition is of higher order, but the hysteresis and long equilibrium times support classification of the transition as one of first order. Bean and Rodbell[27] have presented a model for first-order magnetic transitions, in which the transition is shifted to higher temperatures as a consequence of the exchange interactions' dependence on interatomic distances and the volume change at the transition. According to their model the transition should revert at a lower temperature, which should also provide a better estimate of the magnetic interactions than the transition temperature on heating. We have also found that CrAs transforms back at 253 K, or 6 K below the value determined on heating, and see the unusual shape of the heat-capacity curve as an indication of slow volume-dependent processes.

It is noteworthy that the considerable volume contraction on heating (about 2.1 per cent according to Kazama and Watanabe[10] and about 3 per cent according to Boller and Kallel[13]) does not result in a clearly different non-transitional heat capacity below and above the transition. Thus, the suggestions by Boller and Kallel[13] of differences in vibrational properties as the energetic reason for the transition seem unfounded. Their suggestion that the presence of localized electronic states in the low-temperature state is related to the occurrence of one larger Cr—Cr distance (314.3 pm at 90 K compared with 301.0 pm at 285 K) was not supported by the closely concordant distances found by Selte *et al.*[12] (306.4 pm at 80 K and 303.0 pm at 293 K). As judged from the size of the localized moment only a fraction of the 3d-electrons appear to be localized in the low-temperature phase, and a partly collective behavior is evidenced by the electrical conductivity of CrAs. Kazama and Watanabe[10] reported an almost linear increase in resistivity from $1.7 \times 10^{-4}\,\Omega$ cm at 100 K to $7 \times 10^{-4}\,\Omega$ cm at 250 K. Above the transition the resistivity remained practically constant ($6.5 \times 10^{-4}\,\Omega$ cm). Busch and Hulliger[28] ascribed semiconducting properties to CrAs, while Selte *et al.*[12] found that the diffuse reflectance decreased uniformly in the range 240 to 2000 nm, and thus gave no indication of semiconducting properties.

The electrical properties of CrAs are thus not much changed by the structural change from one MnP-type arrangement into another, but as evidenced by the increasing magnetic susceptibility, the changed band structure allows more readily for population of excited electronic states. The band-structure picture is still not advanced beyond the qualitative stage,[13] and further refinements are needed.

HIGHER-TEMPERATURE REGION

In the absence of a good heat-capacity model for CrAs, its lattice heat capacity was derived from an estimate of the effective Debye temperature in the lower-temperature region and application of a dilational heat-capacity term. The constant Debye temperature used for calculating C_V(lattice) in the harmonic approximation in the higher-temperature region was taken as the maximum of θ_D in a plot against temperature. It turned out to be $\theta_D = 370$ K. According to Grüneisen[29] the dilational heat capacity is

$$C(\mathrm{d}) = C_p - C_V = \alpha\Gamma C_V T, \tag{3}$$

where α is the expansion coefficient, Γ the Grüneisen parameter, C_V the heat capacity at constant volume, and T the thermodynamic temperature. The Grüneisen parameter ($\Gamma = \alpha V/\kappa C_V$), where V is the molar volume and κ is the isothermal compressibility, is not known exactly for CrAs since its compressibility has not been determined, but $\Gamma = 2$ is assumed on the basis of values for related compounds. The volume expansion coefficient, taken from the X-ray work by Selte and Kjekshus[14] is rather large and results in a considerable dilational contribution from 300 K and up to the MnP- to NiAs-type transition temperature. Even so, a large discrepancy exists between the calculated and observed heat capacity at constant pressure, which we attribute to the population of excited electronic states in chromium, amounting to about 1.1 cal_{th} K^{-1} mol^{-1} at 500 K and 1.9 cal_{th} K^{-1} mol^{-1} at 1000 K.

In a regular octahedral ligand field the $^4A_{2g}$ term is always lowest, and the four-fold spin degeneracy and the correspondingly high-spin entropy is therefore expected to persist to low temperatures. This energetically unfavorable low-temperature situation is obviously circumvented by the deformation characteristics of the MnP-type structure. The observed excess heat capacity is compatible with a 1,1 Schottky excitation in the intermediate temperature range, followed by another excitation which we relate to the ^2E_g term.

The best fit was obtained with the following levels and degeneracies: ($|E(hc)^{-1}/cm^{-1}$, $g|$); |0, 2|; |900, 2|; |400, 4|. The curve is shown in figure 3 and the fit is good between 400 and 800 K. Below 400 K residual ordering probably contributes to the heat capacity since the actual $\Delta S_t = 0.69$ cal_{th} K^{-1} mol^{-1} is so much lower than the

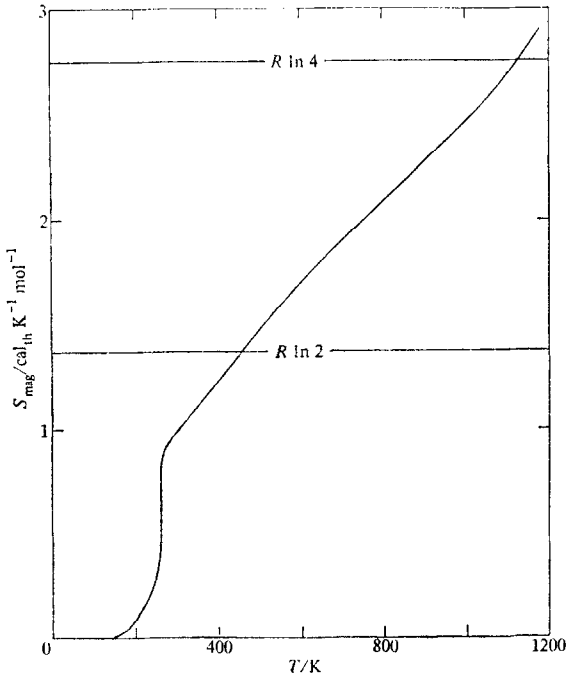

FIGURE 5. Total magnetic entropy of CrAs.

expected value $R \ln 2 = 1.38\ \mathrm{cal_{th}\ K^{-1}\ mol^{-1}}$, see figure 5. In the region above 800 K the transition from the MnP- to the NiAs-type structure contributes to the heat capacity. The transition appears to be continuous, that is without observable isothermal energy absorption on heating. The non-transitional heat capacity in this region was estimated as a sum of vibrational, dilational, and Schottky contributions, and the resulting transitional enthalpy and entropy are $\Delta H_t = 280\ \mathrm{cal_{th}\ mol^{-1}}$ and $\Delta S_t = 0.22\ \mathrm{cal_{th}\ K^{-1}\ mol^{-1}}$. The continuous nature of the transition accords with the theoretical analysis by Franzen *et al.*[30] that according to the Landau theory the transition from the MnP- to the NiAs-type structure can be of second order.

In the region above the transition the heat capacity decreases to about $15.7\ \mathrm{cal_{th}\ K^{-1}\ mol^{-1}}$, which is probably due to the smaller dilational and magnetic contributions in this region. Selte and Kjekshus[14] found that the volume expansion is less pronounced above the transition, and a proportionally smaller dilational heat capacity contribution is indicated in figure 3. Below the transition a 2,2,4 Schottky heat-capacity contribution was assumed, but above the transition a 4,4 contribution is anticipated since in the octahedral field of the NiAs-type structure the $^4A_{2g}$ state might not be split. The magnetic heat-capacity contribution in this range is, therefore, approximated by the following levels and degeneracies ($|E(hc)^{-1}/\mathrm{cm^{-1}}$, g|); |0, 4|; |2400, 4|, see figure 3. The experimentally derived heat capacities above the transition agree with this estimate within their limited accuracy.

The authors appreciate the partial financial support of the National Science Foundation, Björn Lyng Nielsen's assistance at Oslo with the preparation and measurement, and are grateful to Kungliga Fysiografiska Sällskapet for provision of a travel grant for Bengt Falk, as well as to the Brazilian Research Council (CNPq) and the Universidade Federal de Santa Catarina for travel and support for Affonso Alles.

REFERENCES

1. Nowotny, H.; Årstad, O. *Z. Phys. Chem.* **1938,** B38, 461.
2. Haraldsen, H.; Nygaard, E. *Z. Elektrochem.* **1939,** 45, 686.
3. Yuzuri, M. *J. Phys. Soc. Jpn* **1960,** 15, 2007.
4. Hollan, L.; Lecocq, P.; Michel, A. *Compt. Rend. Paris* **1965,** 260, 2233.
5. Boller, H.; Nowotny, H. *Monatsh. Chem.* **1965,** 96, 852.
6. Boller, H.; Wolfsgruber, H.; Nowotny, H. *Monatsh. Chem.* **1967,** 98, 2356.
7. Sobczak, R.; Boller, H.; Bittner, H. *Monatsh. Chem.* **1968,** 99, 2227.
8. Sobczak, R.; Boller, H.; Nowotny, H. paper presented at *III. International Conference on Solid Compounds of Transition Elements.* University of Oslo: Oslo. **1969,** p. 154.
9. Watanabe, H.; Kazama, N.; Yamaguchi, Y.; Ohashi, M. *J. Appl. Phys.* **1969,** 40, 1128.
10. Kazama, N.; Watanabe, H. *J. Phys. Soc. Jpn* **1971,** 30, 1319.
11. Kazama, N.; Watanabe, H. *J. Phys. Soc. Jpn* **1971,** 31, 943.
12. Selte, K.; Kjekshus, A.; Jamison, W. E.; Andresen, A. F.; Engebretsen, J. E. *Acta Chem. Scand.* **1971,** 25, 1703.
13. Boller, H.; Kallel, A. *Sol. State Comm.* **1971,** 9, 1699.
14. Selte, K.; Kjekshus, A. *Acta Chem. Scand.* **1973,** 27, 3195.
15. Sobczak, R.; Boller, H. *IV International Conference on Solid Compounds of Transition Elements.* University of Geneva: Geneva. **1973,** p. 104.
16. Selte, K. Ph.D. Thesis, University of Oslo, Oslo, Norway, 1974.
17. Kallel, A.; Boller, H.; Bertaut, E. F. *J. Phys. Chem. Solids* **1974,** 35, 1139.
18. Mott, N. F. *Proc. Phys. Soc. London* **1949,** A62, 416.
19. Mott, N. F. *Nuovo Cim.* Suppl. 2, **1959,** 7, 312.

20. Goodenough, J. B. *Magnetism and the Chemical Bond.* Interscience: New York and London. **1963.**
21. Hambling, P. G. *Acta Cryst.* **1953,** 6, 98.
22. Westrum, E. F., Jr.; Furukawa, G. T.; McCullough, J. P. Adiabatic low-temperature calorimetry. In *Experimental Thermodynamics,* Vol. 1. McCullough, J. P.; Scott, D. W.: editors. Butterworths: London. **1968.**
23. Grønvold, F. *Acta Chem. Scand.* **1972,** 26, 2216.
24. Grønvold, F. *Acta Chem. Scand.* **1970,** 24, 1036.
25. Smart, J. S. *Effective Field Theories of Magnetism.* W. B. Saunders Co.: Philadelphia and London. **1966.**
26. Sobczak, R. *Monatsh. Chem.* **1974,** 105, 1067.
27. Bean, C. P.; Rodbell, D. S. *Phys. Rev.* **1962,** 126, 104.
28. Busch, G.; Hulliger, F. *Helv. Phys. Acta* **1958,** 31, 301.
29. Grüneisen, E. *Zustand des Festen Körpers, Handbuch der Physik* X. I. Springer: Berlin. **1926.**
30. Franzen, H. F.; Haas, C.; Jellinek, F. *Phys. Rev. B* **1974,** 10, 1248.